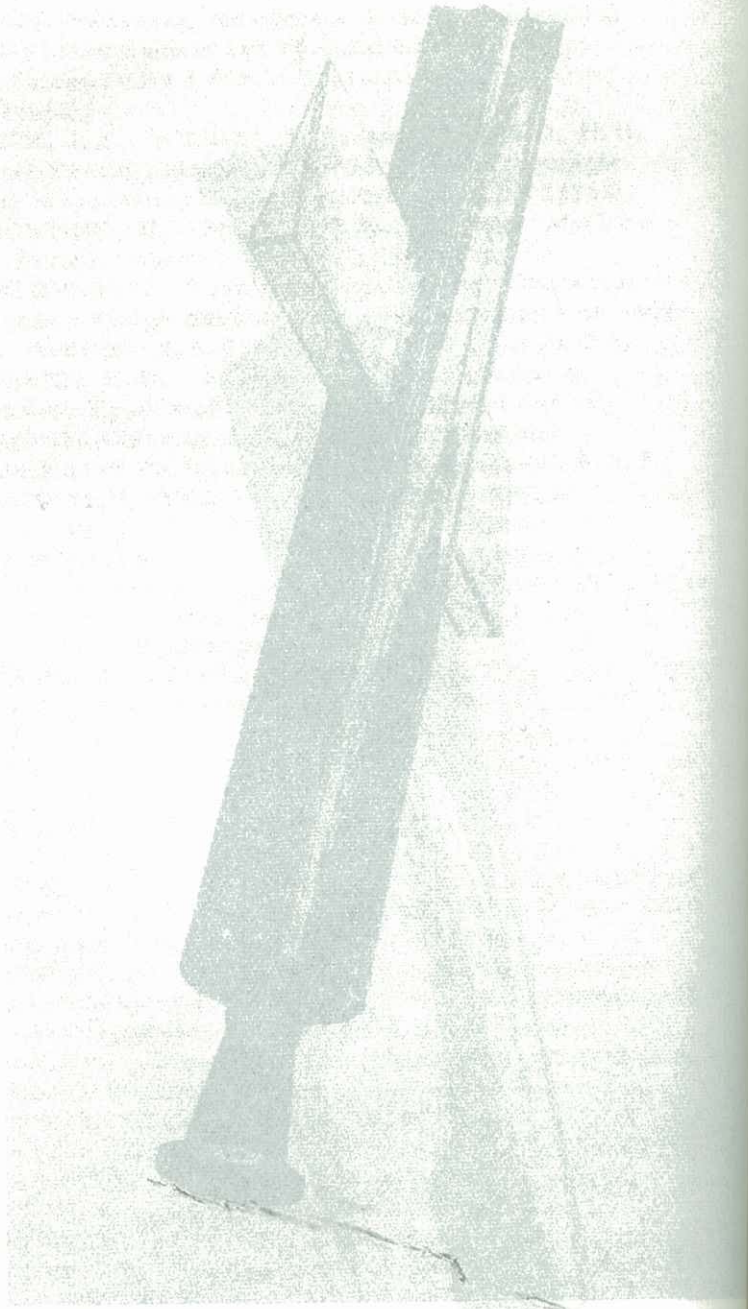

Fig. 3 Photograph of Single Wedge Vane Attachment to Radial Booster.

A GRAPHICAL METHOD TO LOCATE THE ONSET OF CAVITATION

By

M. V. Ramamoorthy,
Scientific Officer
Indian Institute of Science,
Bangalore 12, India

a n d

K. Seetharamaiah,
Associate Professor
Civil and Hydraulics Department
Indian Institute of Science
Bangalore 12, India

A B S T R A C T

This paper presents the results of an experimental investigation on the inception of cavitation in a Quadrant-Edge Orifice meter. The relationship between Reynolds' Number, contraction ratio, and cavitation parameter has been demonstrated under constant back-pressure conditions. Further a graphical method has been suggested for locating exactly the onset of cavitation in a Quadrant-Edge Orifice meter, substantiated with experimental results. This method could as well be applied to other similar pressure differential meters. Values of limiting incipient Reynolds' Numbers are also furnished.

INTRODUCTION: Very few investigators have touched upon the effects of cavitation on metering devices and very little information is available regarding the inception of cavitation in such meters. Hence an attempt has been made to study these ari this paper mainly deals with the inception of cavitation in Quadrant-Edge Orifice meter.

So far, there is no universally accepted simple method for judging the onset of cavitation. The method that is commonly adopted is visual examination of low pressure zones. This is likely to introduce personal errors. Recently, optical, accoustical and electrical methods have been suggested. These methods generally involve the measurements of the effects of cavitation, which are naturally after inception, and the use of very expensive instruments and hence are not encouraging. Further accoustical methods fail sometimes because of the vibration noise and other noises of the power machines used in the system.

SPECIFICATION OF THE METERS USED: The Quadrant-Edge Orifice plates used in the present investigation have the following specifications:

	* β ratio	$\frac{r}{d}$	Manometer tapping
1.	0.225	0.100	D-D/2 tappings
2.	0.400	0.114	,,
3.	0.500	0.135	,,
4.	0.600	0.210	,,
5.	0.630	0.380	,,

*Notations are explained at the end of this paper

EXPERIMENTAL SET-UP: The set up is shown in figure 1. A centrifugal pump of capacity 900 gallons per minute at a head of 120 feet was used to supply the water for the system. Two by-passes of 6" dia. each were used to by-pass the surplus water. The test section consisted of 20 ft. upstream section with 4" dia. G.I. pipe and about 25 ft. downstream section with 4" dia. pipe out of which 4 feet was made of transparent perspex sheet and the rest of G.I. The water was collected in a calibrated collecting tank of capacity of 150 cubic feet.

The downstream end was fitted with a gate valve and a mercury-water differential manometer was used to register the pressure at a point 4" upstream of this gate valve.

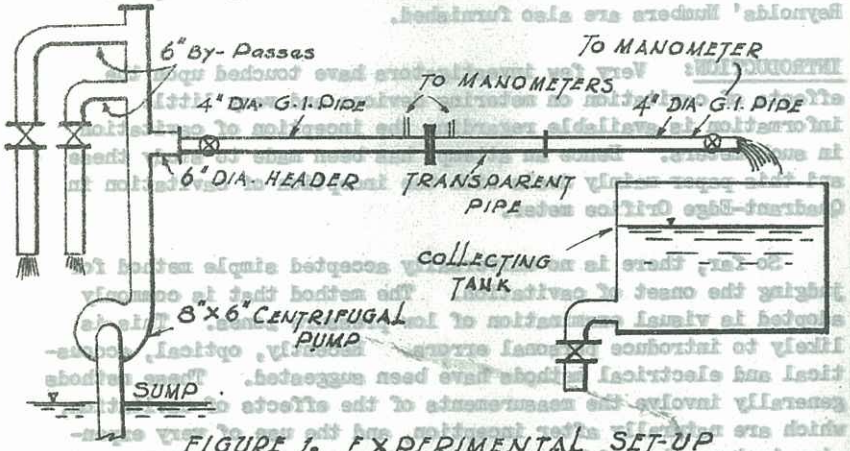

FIGURE 1. EXPERIMENTAL SET-UP

EXPERIMENTAL PROCEDURE AND DATA COLLECTION: Pressures p_1 and p_2 were measured for various discharges keeping p_3 as a constant value. This procedure is repeated for various constant p_3 values (Refer Fig. 2).

The onset of cavitation was determined by hearing the characteristic noise as well as by visual observation for checking the validity of the method suggested.

ANALYSIS OF THE PROBLEM: The problem is solved under the principle of simple hydrodynamic aspect of the flow system. Referring to Figure 2, the dynamic equilibrium between p_1, p_2, p_3 and V_2 completely characterises the flow picture across and downstream of the orifice plate. The combination of p_1, p_2 and V_2 shows up in the discharge coefficient C and so in pipe Reynolds' Number R_D. The downstream conditions can well be represented by p_2 and V_2, if p_3 is kept as a constant quantity in the analysis. Further in order to represent the cavitation conditions, p_2 and V_2 may be combined with p_{Sv}, the saturated vapour pressure to form a cavitation parameter,

$$\sigma = \frac{p_2 - p_{Sv}}{V_2^2/2g} \qquad (1)$$

Hence a plot of pipe Reynolds' Number against σ completely depicts the flow conditions across and downstream of the orifice plate, provided, the back pressure p_3 is kept constant. Since cavitation entails always in loss of energy, there would be an extra loss of energy in the downstream section under cavitating conditions than under noncavitating, other conditions being similar. For a particular Reynolds' Number, therefore, p_2 will

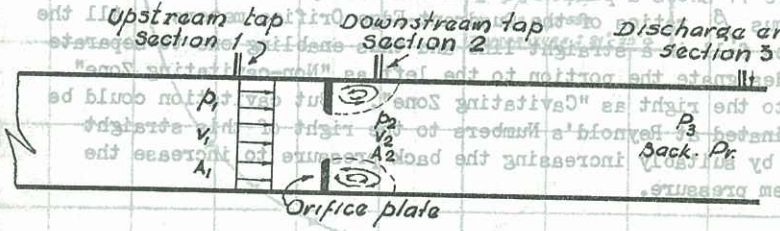

FIGURE 2. DEFINITION SKETCH

be reduced under cavitating conditions, since p_3 is kept constant. The effect of this reduction in p_2 would be to reduce the value of σ. So one can expect a deviation in the plot of σ versus Reynolds' Number under cavitating conditions. Figs. 3, 4, 5 and 6 show a plot of σ against R_D / β^2, under constant back pressures of 0 (atmospheric), 5, 10 and 15 feet respectively. The division of R_D by β^2 is only to get all the data with a single graph for a constant p_3. It seems the cavitation parameter holds more or less the same functional relationship with R_D irrespective of the β ratio, if p_3 is kept constant. Since no significant deviation can be detected from figures 3, 4, 5 and 6, the same data have been plotted in Log-Log scale in figures 7, 8, 9 and 10. It can be seen that the slopes of the straight lines are different under cavitating and noncavitating conditions, with a steeper slope for the latter as per the arguments given above. Obviously the point at which the break occurs represents the conditions at the onset of cavitation. The inception points obtained by visual examination and by hearing the noise are also plotted in the inset block diagrams in each of the figures. It may be noted that these points scatter below the point obtained by the above mentioned graphical solution. This method could be applied to other metering devices as well, since the plots are made to non-dimensional axes.

LIMITING REYNOLDS' NUMBER FOR INCEPTION OF CAVITATION.

The study has been made for various back-pressures and the minimum back-pressure that may be expected in any metering installation is atmospheric and hence, the Reynolds' Number at which the inception of cavitation takes place with free discharge conditions represents the minimum value below which cavitation cannot be expected to occur. This value is different for different β ratio and may be different for other metering devices. Figure 11 shows a plot of such critical Reynolds' Numbers for various β ratios of the Quadrant-Edge Orifice meters. All the points fall in a straight line and thus enabling one to separate and designate the portion to the left as "Non-cavitating Zone" and to the right as "Cavitating Zone". But cavitation could be eliminated at Reynold's Numbers to the right of this straight line by suitably increasing the back pressure to increase the system pressure.

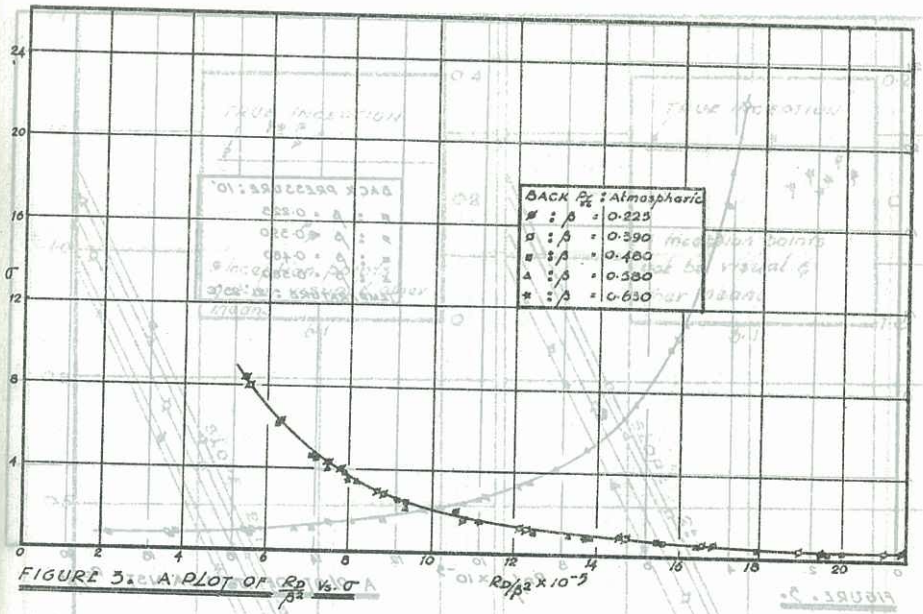

FIGURE 3. A PLOT OF R_D/β^2 Vs. σ

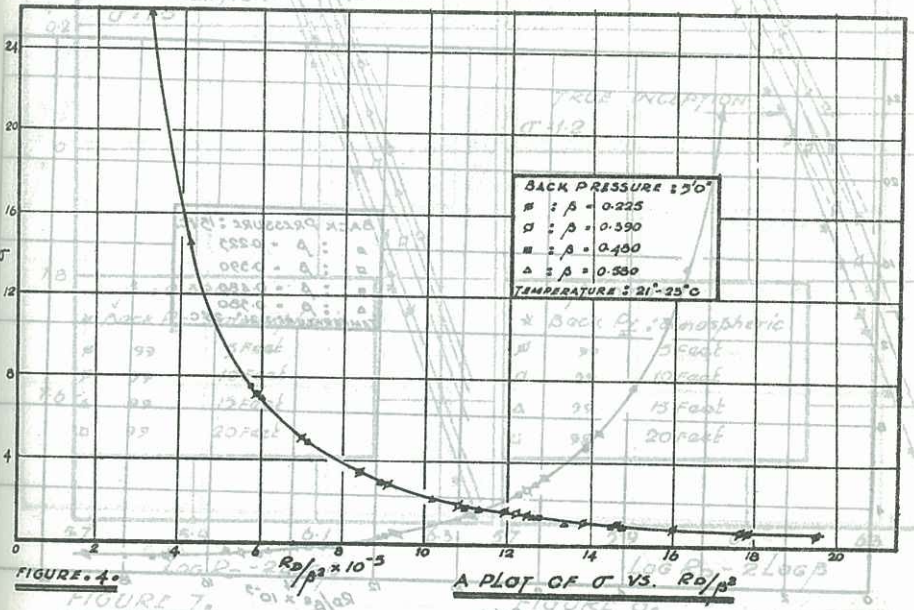

FIGURE. 4. A PLOT OF σ VS. R_D/β^2

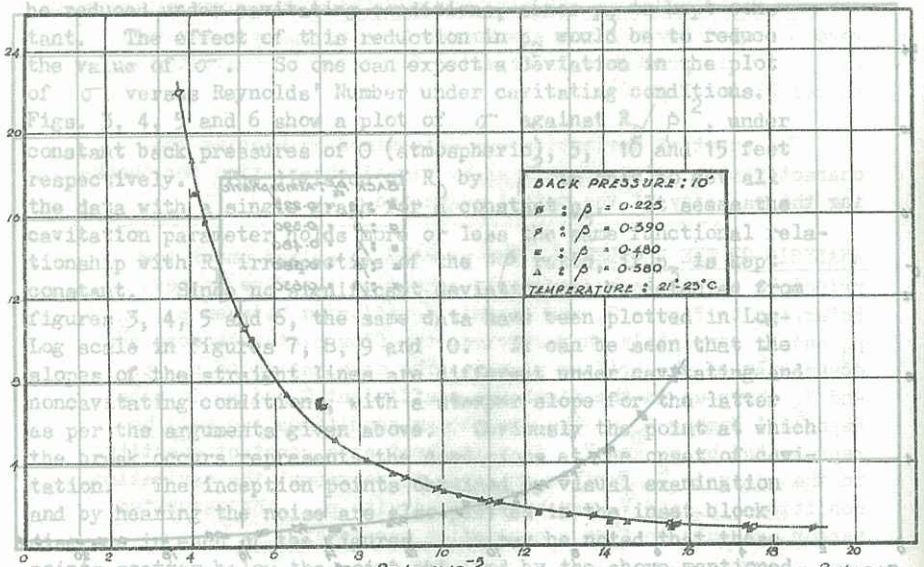

FIGURE. 5. A PLOT OF σ AGAINST R_D/β^2

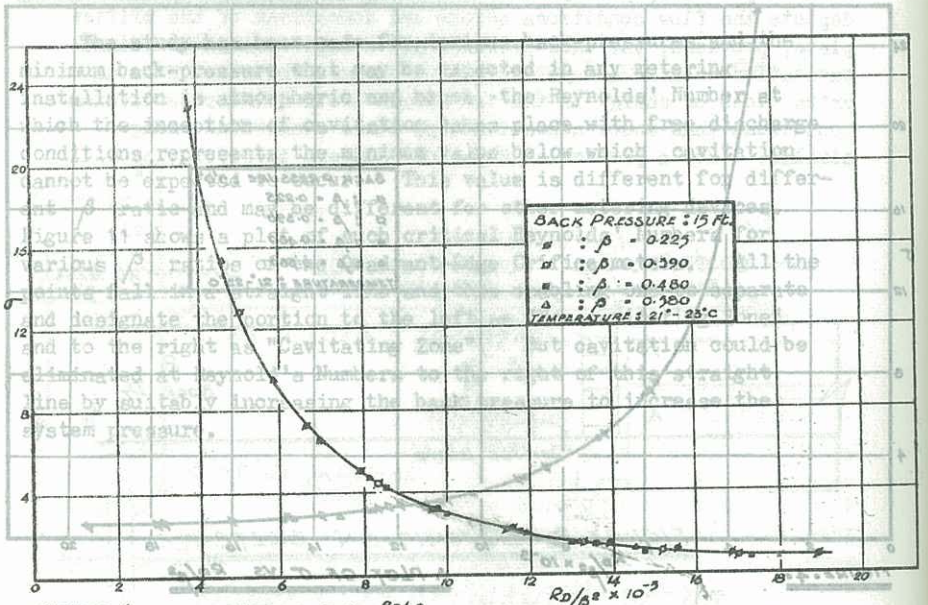

FIGURE 6. A PLOT OF σ Vs. R_D/β^2

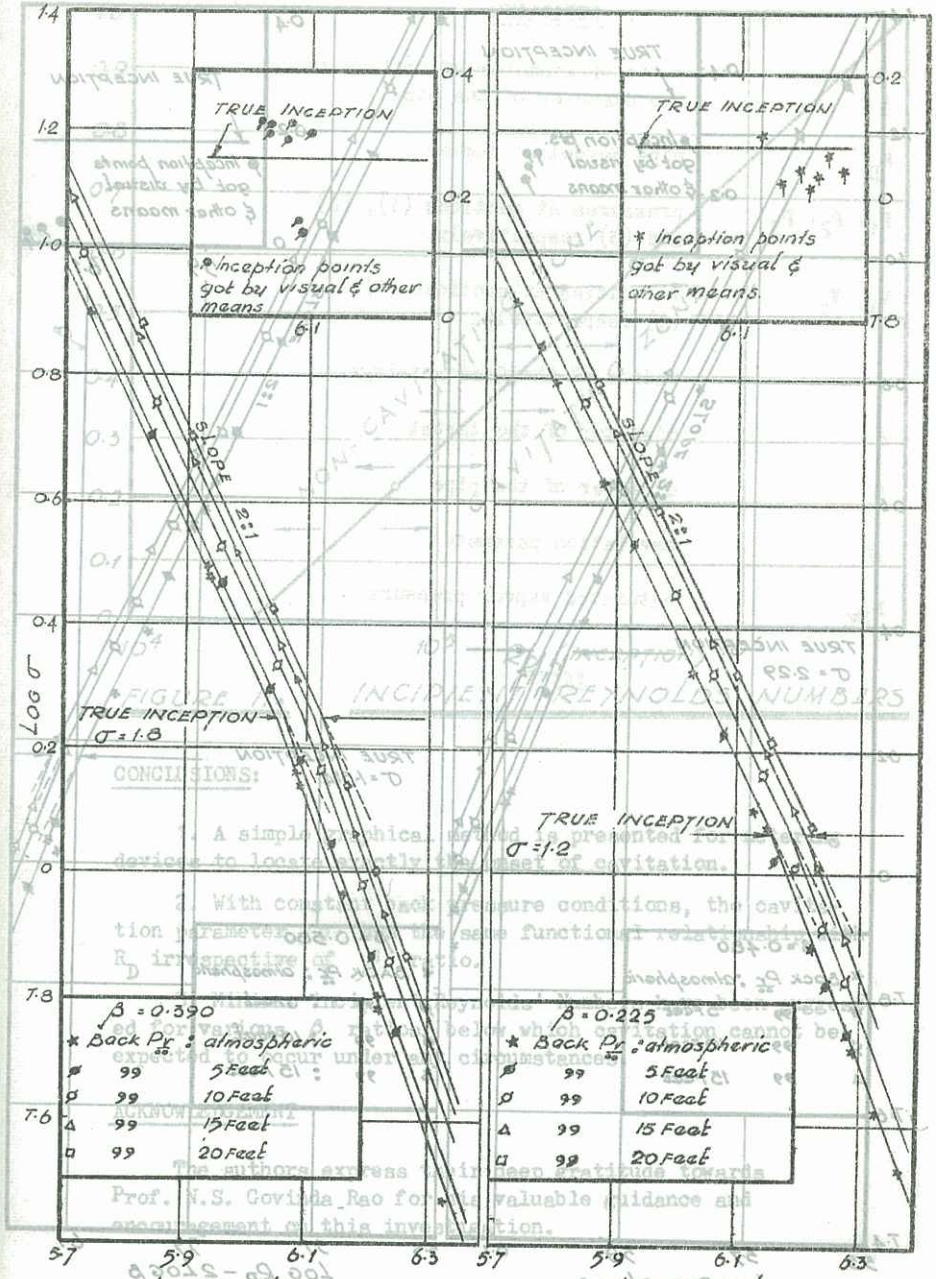

FIGURE 7.

FIGURE 8.

GRAPHICAL METHOD FOR LOCATING INCEPTION

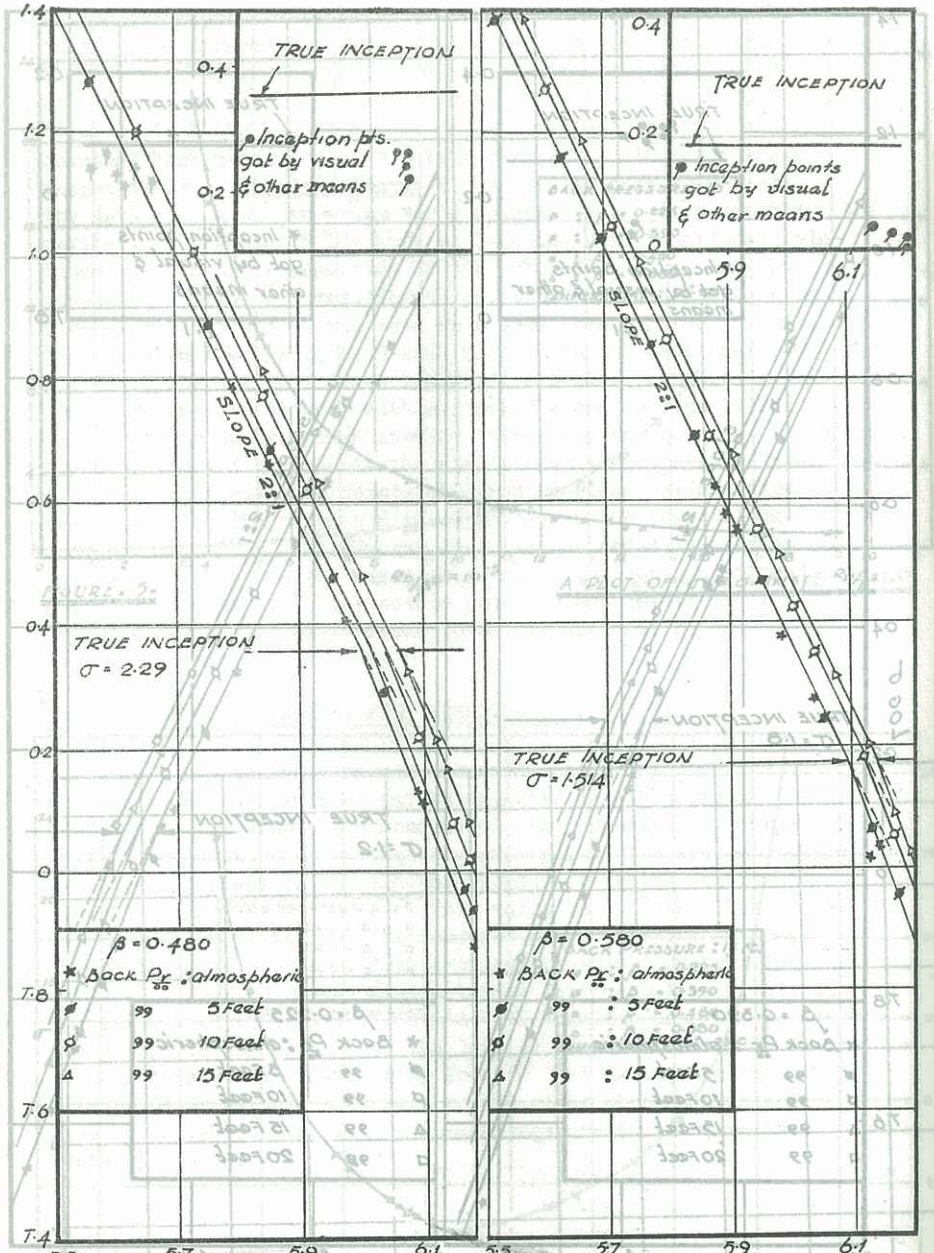

FIGURE 9.

FIGURE 10.

GRAPHICAL METHOD FOR LOCATING INCEPTION.

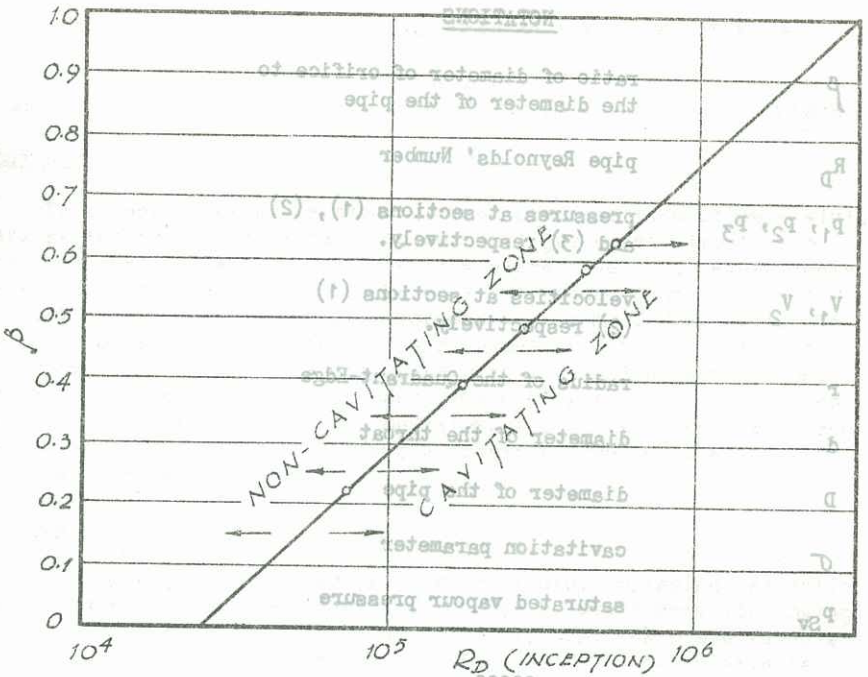

FIGURE 11. INCIPIENT REYNOLDS' NUMBERS

CONCLUSIONS:

1. A simple graphical method is presented for metering devices to locate exactly the onset of cavitation.

2. With constant back pressure conditions, the cavitation parameter σ has the same functional relationship with R_D irrespective of β ratio.

3. Minimum incipient Reynolds' Numbers have been suggested for various β ratios, below which cavitation cannot be expected to occur under any circumstances.

ACKNOWLEDGEMENT

The authors express their deep gratitude towards Prof. N.S. Govinda Rao for his valuable guidance and encouragement on this investigation.

NOTATIONS

β	ratio of diameter of orifice to the diameter of the pipe
R_D	pipe Reynolds' Number
p_1, p_2, p_3	pressures at sections (1), (2) and (3) respectively.
V_1, V_2	velocities at sections (1) (2) respectively.
r	radius of the Quadrant-Edge
d	diameter of the throat
D	diameter of the pipe
σ	cavitation parameter
p_{Sv}	saturated vapour pressure

FIGURE 9.

GRAPHICAL METHOD FOR LOCATING INCEPTION

FIGURE 10.

FLOW BELOW A SUBMERGED SLUICE GATE AS A WALL JET PROBLEM

by N. Rajaratnam
Dept. of Civil Engrg., Univ. of Alberta, Edmonton, Alta., Canada

Abstract:

This paper presents a study of the submerged flow below a sluice gate as the case of a plane turbulent wall jet under almost zero pressure gradient with a backward flow placed over it. Experiments have been conducted for four supercritical Froude Numbers from 3.01 to 6.44 with the submergence factor varying from 1.60 to 2.24. The velocity distribution in the fully developed region follows closely the curve for the classical wall jet with a slight difference only in the scale factors. The boundary shear stress has been measured with a Preston tube. The flow entrainment and the energy fall have also been considered. The appendix presents some calculations for the classical wall jet.

Introduction:

The wall jet is defined as a jet of fluid, impinging tangentially (or at an angle) on a boundary, surrounded by stationary (or moving) fluid. The case of the classical wall jet, i.e. the plane turbulent wall jet issuing into the same stationary fluid of semi-infinite extent, on a smooth boundary, is shown in Fig. 1, in which y_1 is the depth of the slot and U_1 is the velocity which is assumed to be uniform for the entire depth of the slot. A very full discussion of the wall jet problem with an account of the other investigations has been given by Rajaratnam (1,2).

For the classical wall jet, the velocity distribution has been found to be fully developed and similar for $x/y_1 \gtrsim 15$, where x is the longitudinal distance from the slot. The length scale at any section is the normal distance δ from the boundary at which the velocity u is equal to half the maximum velocity u_m, and the velocity gradient $\partial u/\partial y$ is negative. The velocity scale is the maximum velocity u_m at that section. This velocity distribution curve has been finalised by Schwarz and Cosart (3) and Rajaratnam (1) using the available experimental information. The nondimensional distance y/δ is represented by η and the corresponding nondimensional velocity u/u_m by $f(\eta)$.

For the classical wall jet, Sigalla (4) found that

$$\delta/y_1 = 0.5 + 0.065\, x/y_1 \qquad (1)$$

$$u_m/U_1 = 3.45\,(x/y_1)^{-0.50} \qquad (2)$$

τ_o is the boundary shear stress at any section, written as

$$\tau_o = c_f\, \rho\, u_m^2/2 \qquad (3)$$

where c_f is the coefficient of skin friction and ρ is the mass density